Shaping of Thin Grazing-Incidence Reflection Grating Substrates via Magnetorheological Finishing

Ralf K. Heilmann,[a] Mireille Akilian,[a] Chi-Hao Chang,[a] Robert Hallock,[b] Ed Cleaveland,[b] and Mark L. Schattenburg[a]

[a]Space Nanotechnology Laboratory, MIT Kavli Institute for Astrophysics and Space Research, Massachusetts Institute of Technology,
77 Massachusetts Avenue, Cambridge, Massachusetts 02139, USA

[b]QED Technologies, 1040 University Avenue, Rochester, NY 14607, USA

ABSTRACT

Reflection gratings offer high dispersion and thus the potential for high spectral resolution in the soft x-ray band. The requirements of high efficiency and maximum collecting area at minimum mass lead to the desire for densely stacked and exquisitely flat thin-foil grating substrates. In the past we have successfully addressed the problems of thin substrate figure metrology and blazed grating profile fabrication. Our recently developed low-stress thin-foil metrology truss with 50 nm figure repeatability removed a metrology bottleneck and allows us to make progress in the shaping of thin-foil substrates. We present results on the figuring of 100 mm-diameter silicon wafers via magnetorheological finishing to a flatness below 100 nm peak-to-valley, allowing for sub-arcsecond reflection optics.

Keywords: x-ray optics, Constellation-X, reflection gratings, thin-foil optics, figure metrology, magnetorheological finishing, metrology truss

1. INTRODUCTION

Designs for next-generation x-ray telescopes with large collecting area and high spectral resolution, such as Constellation-X,[1] rely on grazing-incidence reflection gratings to provide the necessary high diffraction efficiency and dispersion for soft x-ray photons in the energy range of approximately 0.25 - 2.0 keV (0.6 - 5.0 nm wavelength).[2,3] Maximum throughput at minimal mass calls for reflection gratings that are many centimeters long in the direction of the optical axis of the telescope and less than one millimeter thick. The gratings are placed in the converging beam between the focusing x-ray mirrors and the detector at the telescope focus. The mirror angular resolution of about 10 arcsec or less should not be degraded by the reflection gratings, which requires deviations from flatness to be no more than 2 arcsec or less.[4,5] For low-spatial frequency distortions, such as a single bow traversing the length of the optic, the 2 arcsec limit would require a flatness below 0.5 μm for a 100 mm-long grating.

Inexpensive optic candidates with aspect ratios of length over thickness of ~ 100 are readily available. Examples of such thin-foil optics are glass in the shape of flat panel displays and silicon wafers mass-produced for the semiconductor industry.[6] Both materials also offer good mechanical strength, low density, and low microroughness, but they lack the required flatness. Large glass sheets of sub-mm thickness are often warped by more than their thickness. Their low-frequency figure can be improved through thermal slumping to better than 10 arcsec.[6,7] Silicon wafers often have very good thickness uniformity achieved through double sided polishing. When such a wafer is chucked onto a flat the wafer itself appears very flat. However, in a low-mass, high throughput modular assembly of many reflection gratings chucking to a flat is out of the question. Rather, a grating substrate is desired that *remains flat in the absence of external forces.* Low bow and low warp wafers still deviate ≈ 5 μm from flat in their relaxed state, similar to slumped glass.

The first step in improving the figure of an optic is measurement of the figure, or figure metrology. Once the figure is known one can test means to improve it. The challenge in measuring the figure of thin-foil optics is how

Further author information: Send correspondence to R.K.H. E-mail: ralf@space.mit.edu, URL: http://snl.mit.edu/

Optics for EUV, X-Ray, and Gamma-Ray Astronomy II, edited by Oberto Citterio, Stephen L. O'Dell,
Proc. of SPIE Vol. 5900, 590009, (2005) · 0277-786X/05/$15 · doi: 10.1117/12.617788

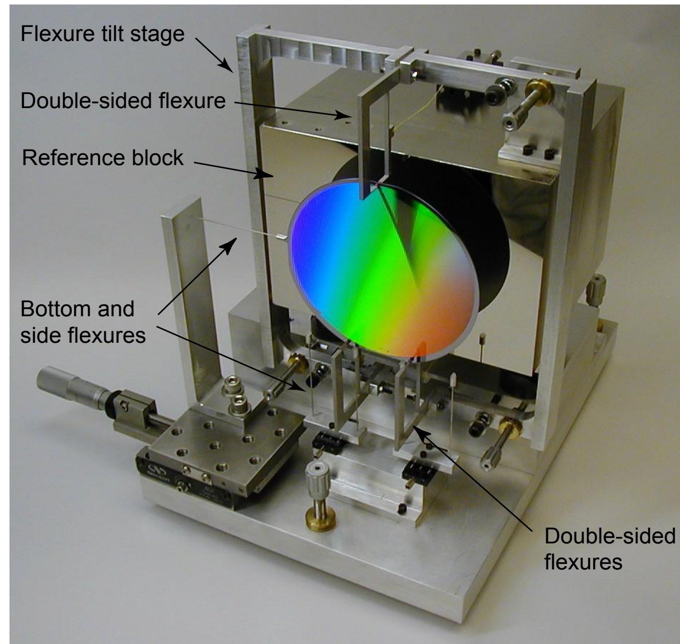

Figure 1. Thin-foil optic metrology truss, holding a 100 mm diameter silicon wafer that is patterned with a 400 nm period resist grating.

to hold them without distorting them. We have analyzed the functional requirements for a holding device and designed a metrology truss that enables us to perform figure measurements with better than 50 nm dynamic repeatability on 100 mm diameter silicon wafers.[8,9]

Figure corrections through traditional optical polishing are very difficult to perform on thin-foil optics. However, Magnetorheological Finishing[10] (MRF) is an optical figuring technique that allows for very predictable material removal on low spatial frequency scales. We have used MRF in the past to flatten silicon wafers from over 6 μm to just below 1 μm non-flatness peak-to-valley (P-V).[11] At the time the lack of sub-μm repeatable figure metrology prevented us from exploring the capabilities of MRF further.

2. THIN-FOIL METROLOGY TRUSS

Our thin-foil metrology truss is shown in Fig. 1, holding a 100 mm-diameter silicon wafer that has been patterned with a 400 nm period grating. The wafer is held in front of a flat reference block by three monolithic double-sided flexures that constrain translation along the optic normal and rotation around vectors lying in the plane of the optic. These flexures each have a moving arm that allows the flexure to open and close for insertion and removal of the optic, and a fixed arm against which the optic comes to rest. Terminated with small ruby balls, the moving and fixed arms oppose each other to minimize local torques on the optic. Two “antenna” flexures support the wafer from below against gravity and constrain rotation about the wafer normal. Another antenna flexure on the side of the wafer serves as a reference for positioning along this direction.

The double-sided flexures are attached to a vertical tilt stage, which in turn is connected to the reference block. The whole truss can be aligned in pitch and yaw relative to the gravity vector through a horizontal tilt stage. An inclinometer mounted to the reference block can be used to monitor pitch and yaw.

The metrology truss was designed to minimize the effects of potentially distorting forces due to gravity, thermal expansion mismatch, and friction between flexures and optic.[8,9] For glass or silicon thin-foil optics of 0.5 mm thickness and $\approx$ 140 mm in diameter we expect the figure of an optic that has been properly mounted and aligned to gravity to deviate from its force-free shape by less than 50 nm based on machining tolerances and the absence of systematic errors.

The dynamic repeatability of the metrology truss was tested through measurement of the surface map of a 100 mm-diameter silicon wafer with a Shack-Hartmann (SH) wavefront sensor,[11,12] removing the wafer from the holder and replacing it, and measuring the surface again. The dynamic repeatability was found to be 55 nm P-V.[9]

3. MAGNETORHEOLOGICAL FINISHING (MRF)

Magnetorheological finishing is a figuring technique with a well-controlled material removal function.[10] Material is removed when the optic is lowered into a stream of magnetorheologic, abrasive carrying fluid that flows over the top of a spherical wheel. The fluid is controlled and "hardened" through a magnetic field gradient in the gap between the spinning wheel and the optic. Due to the quasi-deterministic nature of the removal function, desired figure corrections can be programmed into the polishing algorithm based on the (measured) initial optic shape. In principle the outcome should be insensitive to mounting distortions during MRF.

The experiments described below were performed on a QED Q22-X MRF system, which employs a spiral polishing tool path, working its way in from the edge of the rotating optic to its center.

4. SAMPLES AND EXPERIMENTAL SETUP

As sample optics we used 100 mm diameter, nominally 525 μm thick [100] silicon wafers (n-type Si:P, 1.1 - 1.4 mW/cm resistivity).[13] Maximum warp and bow were specified to be 7.2 and 2.2 μm, respectively. From a box of 25 wafers we selected those with the smallest deviation from flat when held in the metrology truss as measured with our SH wavefront sensor.

For the current experiment the metrology truss was positioned about 17 cm in front of a Zygo 4" GPI XP HR interferometer on an optical table. The temperature was controlled to within $\sim \pm 1$ deg C, and the table was surrounded by a plastic curtain to reduce turbulence. The surface topography data is generated through a phase modulation algorithm. Each data set is an average over 16 measurements, which results in a time average over $\sim$ 10 seconds.

5. RESULTS AND DISCUSSION

5.1. Metrology repeatability

For wafer figure measurements a wafer is inserted into the metrology truss by hand with its main flat resting on the antenna flexures and with the double-sided flexures opened by $\sim$ 1 mm. Lateral positioning is judged by eye, using the side flexure as a reference. We estimate lateral positioning repeatability to be no worse than 0.5 mm. The double sided flexures are then gradually closed while the wafer is ever so slightly "leaning" against the ruby balls of the fixed arms. The weight-supporting bottom flexures are tapped slightly to relieve any potential stress build-up due to friction between the wafer and the flexures before the wafer is pinched between the three pairs of ruby balls in its final position. After the operator steps back and the curtain around the table is closed we wait 1-2 minutes for turbulence to die down and for the interference fringes to stabilize before taking data.

Over the course of these experiments the static measurement repeatability for wafer surface maps was $\sim$ 25 nm P-V and 4 nm rms over an 87 cm diameter aperture and time delays of 5 to 50 minutes between measurements.

The dynamic repeatability was tested by removing and replacing a wafer by different operators. Maps taken over a similar aperture before and after wafer replacement differed by about 50 nm P-V and less than 10 nm rms.

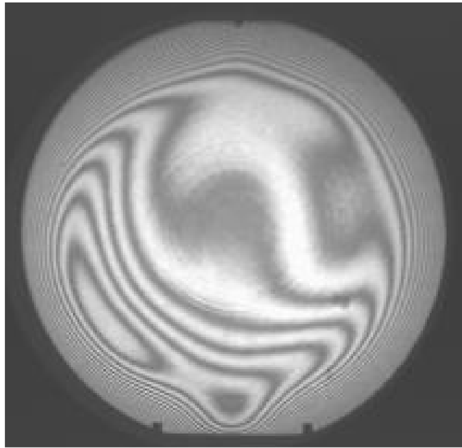

(a) Wafer A pre-MRF

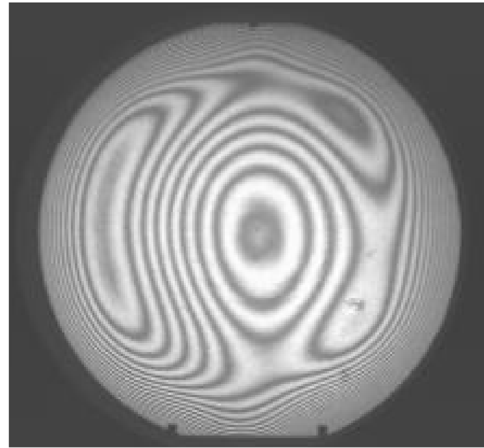

(b) Wafer B pre-MRF

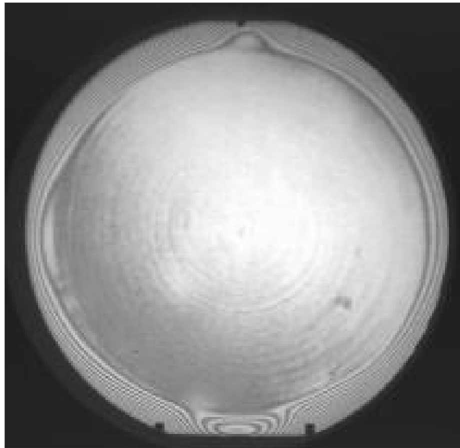

(c) Wafer A post-MRF

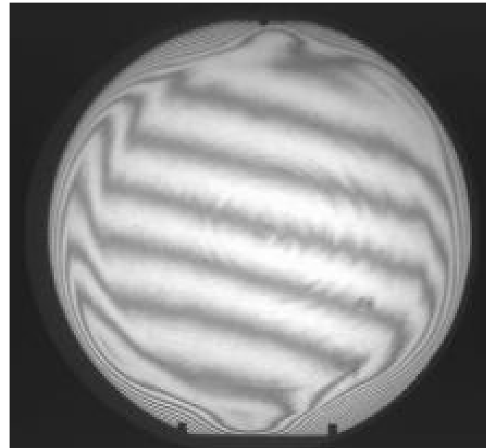

(d) Wafer B post-MRF

Figure 2. Silicon wafer interferograms of (a) wafer A and (b) wafer B as received from the vendor, and of (c) wafer A after three MRF front-side steps and of (d) wafer B after four MRF front-side steps. The interferograms show the full 100 mm-diameter wafers with their main flat at the bottom. The double-sided flexures obscure two small areas at the bottom and one small spot at the top. Wafer B was only figured over the central 75 mm aperture. See text for more details.

5.2. Initial wafer shape

Two wafers (A and B) were used in our experiments. As can be seen from their interferograms in Fig. 2, their surface slope increases towards the edges of the wafers. The topography at the outer ~ 5 mm cannot be resolved by the interferometer. We therefore limited our analysis to circular apertures of 91 mm diameter or less. The initial surface maps of wafer A (B) had P-V and rms values of 3.14 (2.81) and 0.40 (0.56) μm, respectively. Both wafers showed a slight "doughnut" shape with an elevated ring surrounding a bowl-shaped depression. Both wafers also displayed curious circular grooves of up to 20 nm amplitude and of roughly 5 mm period on both sides before any MRF. The grooves resemble patterns formed by so-called swirl defects created during crystal growth.[14] We speculate that these defects might give rise to the observed grooves during the lapping and polishing in the wafer manufacturing process.

5.3. Magnetorheological finishing

Wafer A was polished first, removing about 3 μm of material from the high spots. The removal happens over an area (tool "footprint" or "spot") of about 4.25 mm wide by 9.8 mm long, while the wafer rotates around its center at variable speed.

After the first polishing step the wafer showed a significant spherical distortion (akin to the power of a lens) of $\sim 1\mu$m. This is typical for thin optics if there was stress present in the removed material. Even though our silicon wafers are single crystals they apparently are stressed during manufacture. In order to "balance" the stress distribution we removed a 200 nm layer of constant thickness from the back of the wafer. This second MRF step basically removed the spherical distortion, resulting in a surface of 0.71 μm P-V and 80 nm rms over a 85 mm aperture.

The next MRF step on the front of wafer A cut those values roughly in half. The third MRF front polish led to a small spherical distortion (power ~ 100 nm). After removal of another 100 nm from the back the power term was basically eliminated. The 0.32 μm P-V of the resulting front surface map is dominated by edge features and a low spot in the center. However, the rms over an 85 mm aperture is a remarkable 18 nm. Shrinking the aperture to 81 mm the P-V value reduces to 0.18 μm. The 0.1 μm low spot could presumably best be eliminated by further material removal with a raster-scan MRF tool.

With the experience gained from Wafer A we decided to start MRF on wafer B with a constant removal of 300 nm from the back, followed by a front-side polish based on the surface map taken before the back-side removal. This treatment resulted in a surface map with deviations from flat below 0.5 μm P-V and about 80 nm rms over a 75 mm aperture, and no discernible power term. Due to the strongly sloped, low-lying areas around the rim of the wafer that would require additional removal of $\sim 1\mu$m over most of the wafer we decided to only polish over a 75 mm aperture from then on. The next three successively shorter MRF steps led to progressively smaller P-V and rms values, with the final result being 74 nm P-V and 10 nm rms over a 75 mm aperture. The total MRF time for wafer B was under 4 hours.

Despite the circular grooves that are now clearly visible, the slope distribution has an rms of ~ 1.3 arcsec (see Fig. 3). Like most figuring and polishing techniques MRF is not well suited to remove figure errors with spatial frequencies comparable to the inverse of the spot or tool size, as is the case with the swirling grooves here. MRF can be performed with a smaller spot size, but at the cost of a reduced material removal rate. Without these grooves wafer B would represent an optic with sub-arsec (FWHM) deviations from flat. We will explore the availability of silicon wafers without such grooves.

5.4. Microroughness

Surface roughness was measured with a white light interferometer and an atomic force microscope (AFM). The roughness values before any MRF were in the range of 0.1 - 0.3 nm, and between 0.13 and 0.7 nm after various MRF steps. Ignoring the single 0.7 nm measurement the average from the post-MRF white light interferometer measurements was 0.34 ± 0.1 nm and 0.22 ± 0.08 nm from the AFM measurements.

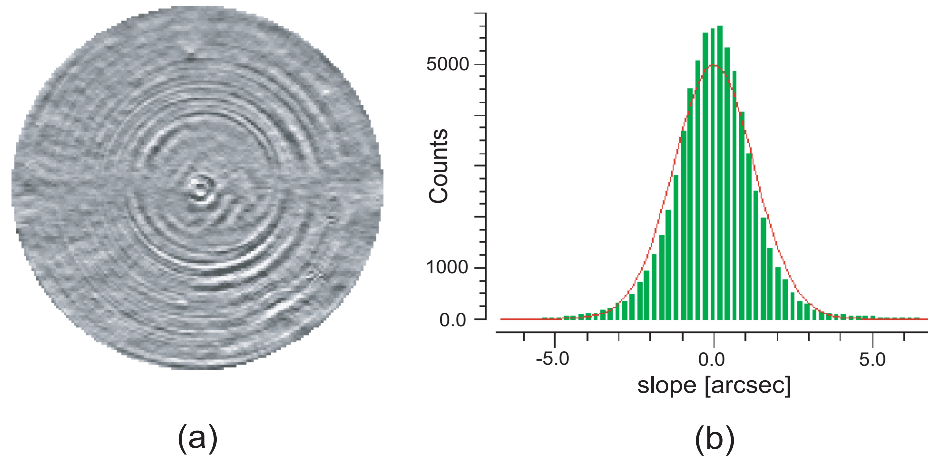

Figure 3. Wafer B after four MRF front side steps. (a) Surface slope map over a 75 mm aperture, showing the swirl pattern. (b) Slope histogram with Gaussian fit. See text for details.

5.5. Alignment to gravity vector

No measures were taken during metrology to ensure that the gravity vector was in the plane of the wafer front surface. It is therefore expected that there was a small, but constant angle between the wafer normal and the horizontal plane (defined to be the plane normal to the local gravity vector). If the magnitude of this angle was 100 arcsec a perfectly flat wafer would be expected to bow by an amount that is small compared to the dynamic repeatability of our setup. The reference block is equipped with an inclinometer with 18 arcsec resolution and 36 arcsec repeatability in both pitch and yaw. We plan to perform self-calibration tests to establish accurate alignment of the reference flat with respect to gravity, which in turn will enable alignment of the thin-foil optic to gravity as well.[9]

6. SUMMARY AND OUTLOOK

We have demonstrated the feasibility of flattening thin-foil optics in a quasi-stress-free state to arcsec precision. The two main ingredients for this achievement are the ability to perform ultra-low-deformation metrology on the thin-foil optic and the availability of a deterministic figuring process. We were able to hold silicon wafers with 50 nm P-V dynamic repeatability in our metrology truss. With one backside and four front side MRF steps we reduced wafer non-flatness from 2.81 μm to 75 nm P-V.

We have shown that sub-arcsecond thin-foil optics with aspect ratios of ~ 200 should be achievable with current technology. However, in order to produce the large areas necessary for future x-ray spectroscopy telescopes at minimal cost it is crucial to aggressively preselect or prepare substrates with small figure errors, since large figure corrections over large areas make MRF time consuming and expensive.

ACKNOWLEDGMENTS

We gratefully acknowledge technical support from R. C. Fleming at the Space Nanotechnology Laboratory, interferometer software from S. R. Kobak at Zygo, and helpful conversations with B. Zheng at Wafer World. This work is supported by NASA grants NAG5-12583 and NAG5-5405.

REFERENCES

1. H. Tananbaum, N. White, J. Bookbinder, R. Petre, and K. Weaver, "Constellation X-Ray Mission: Recent developments for mission concept and technology development," in *UV and Gamma-Ray Space Telescope Systems*, G. Hasinger and M. J. L. Turner, eds., *Proc. SPIE* **5488**, pp. 492–504, 2004.
2. K. A. Flanagan *et al.*, "The Constellation-X RGS options: Raytrace modeling of the off-plane gratings," in *UV and Gamma-Ray Space Telescope Systems*, G. Hasinger and M. J. L. Turner, eds., *Proc. SPIE* **5488**, pp. 515–529, 2004.
3. R. A. Cameron *et al.*, "Generation-X: Mission and technology studies for an x-ray observatory vision mission," in *UV and Gamma-Ray Space Telescope Systems*, G. Hasinger and M. J. L. Turner, eds., *Proc. SPIE* **5488**, pp. 572–580, 2004.
4. S. M. Kahn *et al.*, "Large-area reflection grating spectrometer for the Constellation-X mission," in *EUV, X-Ray, and Gamma-Ray Instrumentation for Astronomy X*, O. H. W. Siegmund and K. A. Flanagan, eds., *Proc. SPIE* **3765**, pp. 94–103, 1999.
5. W. C. Cash and A. F. Shipley, "Off-plane grating mount tolerances for Constellation-X," in *UV and Gamma-Ray Space Telescope Systems*, G. Hasinger and M. J. L. Turner, eds., *Proc. SPIE* **5488**, pp. 335–340, 2004.
6. R. K. Heilmann, G. P. Monnelly, O. Mongrard, N. Butler, C. G. Chen, L. M. Cohen, C. C. Cook, L. M. Goldman, P. T. Konkola, M. McGuirk, G. R. Ricker, and M. L. Schattenburg, "Novel Methods for Shaping Thin-Foil Optics for X-Ray Astronomy," in *X-Ray Optics for Astronomy: Telescopes, Multilayers, Spectrometers, and Missions*, R. B. Hoover and P. Gorenstein, eds., *Proc. SPIE* **4496**, pp. 62–72, 2002.
7. R. Petre, D. A. Content, J. P. Lehan, S. L. O'Dell, S. M. Owens, W. A. Podgorski, J. W. Stewart, and W. W. Zhang, "Recent progress on the Constellation-X spectroscopy x-ray telescope (SXT)," in *Optics for EUV, X-Ray, and Gamma-Ray Astronomy*, O. Citterio and S. L. O'Dell, eds., *Proc. SPIE* **5168**, pp. 196–206, 2004.
8. R. K. Heilmann, M. Akilian, C.-H. Chang, C. R. Forest, C. Joo, A. Lapsa, J. C. Montoya, and M. L. Schattenburg, "Thin-foil reflection gratings for Constellation-X," in *UV and Gamma-Ray Space Telescope Systems*, G. Hasinger and M. J. L. Turner, eds., *Proc. SPIE* **5488**, pp. 283–290, 2004.
9. M. Akilian, C. R. Forest, A. H. Slocum, D. L. Trumper, and M. L. Schattenburg, "Thin optic constraint," submitted to *Precision Engineering*, 2004.
10. W. Kordonski and D. Golini, "Progress update in magnetorheological finishing," *Int. J. Mod. Phys. B* **13**, pp. 2205–2212, 1999.
11. C. R. Forest, M. L. Schattenburg, C. G. Chen, R. K. Heilmann, P. T. Konkola, J. Przbylowski, Y. Sun, J. You, S. M. Kahn, and D. Golini, "Precision shaping, assembly, and metrology of foil optics for x-ray reflection gratings," in *X-ray and Gamma-ray Telescopes and Instruments for Astronomy*, J. E. Trümper and H. D. Tananbaum, eds., *Proc. SPIE* **4851**, pp. 538–548, 2003.
12. C. R. Forest, C. R. Canizares, D. R. Neal, M. McGuirk, A. H. Slocum, and M. L. Schattenburg, "Metrology of thin transparent optics using Shack-Hartmann wavefront sensing," *Opt. Eng.* **43**, pp. 742–753, 2004.
13. Wafer World, West Palm Beach, FL 33407, http://www.waferworld.com/
14. H. Föll and B. O. Kolbesen, "Formation and nature of swirl defects in silicon," *Appl. Phys.* **8**, pp. 329–332, 1975.